

The effect of aberrated recording beams on reflecting Bragg gratings

Marc SeGall*, Daniel Ott, Ivan Divliansky, and Leonid B. Glebov
CREOL – The College of Optics & Photonics, University of Central Florida, P.O. Box 162700
Orlando, FL USA 32816-2700

Keywords: aberrations, volume gratings, holographic optical elements

ABSTRACT

The effect of aberrations present in the recording beams of a holographic setup is discussed regarding the period and spectral response of a reflecting volume Bragg grating. Imperfect recording beams result in spatially varying resonant wavelengths and the side lobes of the spectrum are washed out. Asymmetrical spectra, spectral broadening, and a reduction in peak diffraction efficiency may also be present, though these effects are less significant for gratings with wider spectral widths.

Reflecting Bragg gratings (RBGs) are used as elements in a variety of applications including spectral beam combining^{1,2}, mode locking^{3,4}, longitudinal and transverse mode selection in lasers^{5,6}, and sensing^{7,8}. For applications requiring narrow spectral selectivity⁹, or large apertures¹⁰, these gratings must have a uniform period throughout the length of the recording medium, which may be on the order of millimeters. However, when using typical recording techniques such as two-beam interference for large aperture gratings and phase-mask recording of fiber gratings, aberrations from the optical elements in the system result in an imperfect grating structure¹¹⁻¹³. In this paper we consider the effects of aberrations on large aperture gratings recorded in thick media using the two-beam interference technique. Previous works in analyzing the effects of aberrations have considered the effects of aberrations in a single recording plane where the beams perfectly overlap. Such an approach is valid for thin media (on the order of tens of microns), but for thick recording media (on the order of several millimeters) there will be a significant shift in the positions of the beams relative to each other as they traverse the recording medium. Therefore, the fringe pattern produced will not be constant throughout the grating if one or both beams have a non-uniform wavefront. Such non-uniform gratings may have a wider spectral width, a shifted resonant wavelength, or other problems. It is imperative therefore to know what the effects of aberrations will have on the properties of the RBGs. Thus, in this paper we consider the imperfect fringe pattern caused by the recording beams and its effect on the diffraction efficiency and spectral profile of the recorded reflecting volume Bragg gratings.

Let us consider two aberrated beams which interfere at a recording medium as shown in Fig. 1. The intensity profile is given by the well-known two-beam interference equation

(1)

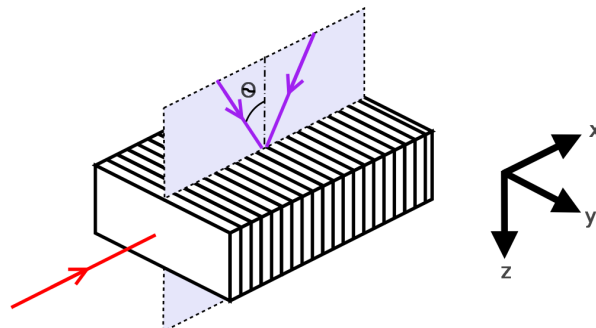


Fig. 1: Recording and reconstruction geometries. The recording beams are incident at an angle θ , and the probe beam is at normal incidence to the grating face.

*msegall@creol.ucf.edu

$$I(x, y) = I_1(x, y) + I_2(x, y) + 2\sqrt{I_1(x, y)I_2(x, y)} \cos\left(\left(\bar{k}_1 - \bar{k}_2\right) \cdot \bar{r} + \varphi_1(x, y) - \varphi_2(x, y)\right),$$

where I_j , k_j , and φ_j are the intensity, wave vector, and aberration contribution of each beam, respectively. In a typical recording geometry, a single beam is split into the two recording beams and each beam is reflected towards the recording medium, which bisects the angle between the mirrors. As high quality beamsplitters and mirrors are commercially available we will assume that any aberrations are produced prior to the beamsplitter, during beam shaping or resizing. In this case $\varphi_2(x, y) = \varphi_1(-x, y)$ and Eq. 1 can be rewritten as

$$I(x, y) = I_1(x, y) + I_2(x, y) + 2\sqrt{I_1(x, y)I_2(x, y)} \cos(2kx \sin \theta + \varphi_1(x, y) - \varphi_1(-x, y)). \quad (2)$$

Here k is the wavenumber and θ is the angle of incidence in the medium. To determine the effects of a shifting fringe pattern, consider the case of a uniform beam of radius r , split as described previously, with each of the split beams interfering in a thick recording medium. Generally the centers of the beams will not overlap (except in one particular z -plane). Defining the plane $z = 0$ as the plane where the beam centers overlap Eq. 2 becomes

$$I(x, y, z) = I_1(x + z \tan \theta, y) + I_2(x - z \tan \theta, y) + 2\sqrt{I_1(x + z \tan \theta, y)I_2(x - z \tan \theta, y)} \cos(2kx \sin \theta + \varphi_1(x + z \tan \theta, y) - \varphi_1(z \tan \theta - x, y)) \quad (3)$$

In order to properly describe the aberrations in this system, we will write the aberrations in terms of Zernike polynomials, which will allow us to characterize the aberrations of the recording beam with a unique, orthogonal expansion¹⁴. As the Zernike polynomials are normalized to the radius of the aperture of interest, r , we will denote the normalized dimensions as follows:

$$x' = \frac{x}{r} \quad y' = \frac{y}{r} \quad z' = \frac{z}{r}.$$

The first few Zernike polynomials are listed in Table 1. The effect of aberrations on the wavefront is thus

$$\varphi_1(x' + z' \tan \theta, y') - \varphi_1(z' \tan \theta - x', y') = 2\pi \sum_n c_n Z_n^*(x', y'; z'), \quad (4)$$

Table 1: Zernike polynomials, their Cartesian form, and their effect on the wavefront.

Zernike Polynomial	Aberration	Cartesian Form of Z_n	Z_n^*
0	Piston	1	0
1	Tilt x	x'	$2x'$
2	Tilt y	y'	0
3	Defocus	$2(x'^2 + y'^2) - 1$	$8x'z' \tan \theta$
4	0° Astigmatism	$x'^2 - y'^2$	$4x'z' \tan \theta$
5	45° Astigmatism	$2x'y'$	$4x'y'$
6	Coma x	$3x'^3 + 3x'y'^2 - 2x'$	$2x'(9z'^2 \tan^2 \theta + 3x'^2 + 3y'^2 - 2)$
7	Coma y	$3x'^2 y' + 3y'^3 - 2y'$	$12x'y'z' \tan \theta$
8	30° Trefoil	$x'^3 - 3x'y'^2$	$2x'(3z'^2 \tan^2 \theta + x'^2 - 3y'^2)$
9	0° Trefoil	$3x'^2 y' - y'^3$	$12x'y'z' \tan \theta$
10	Spherical	$6(x'^4 + y'^4 - x'^2 - y'^2) + 12x'^2 y'^2 + 1$	$24x'z' \tan \theta (2z'^2 \tan^2 \theta + 2x'^2 + 2y'^2 - 1)$

where $Z_n^*(x', y', z') = Z_n(x' + z' \tan \theta, y') - Z_n(z' \tan \theta - x', y')$, Z_n is the n th Zernike polynomial and c_n is the coefficient of the n th polynomial, chosen to give units of waves inside the recording medium. The contributions of each individual aberration are listed in Table 1. Note that while there is a contribution to the wavefront due to tilt, we will ignore it here as any tilt in the beam can be compensated by adjusting the angle of interference.

By grouping terms in Eq. 4 that have the same dependence on x we can rewrite the modulation term of Eq. 3 as follows:

$$\cos\left(2kx \sin \theta + 2\pi \sum_n c_n Z_n^*(x', y', z')\right) = \cos\left(\sum_{n=1,3,\dots} p_n(y', z') x^n\right) = \cos\left(\frac{2\pi}{\Lambda} x\right). \quad (5)$$

Here $p_1(y', z')$ is the sum of all terms with a linear dependence on x (including the term forming the original, unaberrated grating), $p_3(y', z')$ is the sum of all terms with a cubic dependence on x , etc. (from the symmetry of the system all terms with even powers of x will be canceled). The grating period Λ is thus equal to

$$\Lambda(x, y, z) = \frac{2\pi}{\sum_{n=1,3,\dots} p_n(y', z') x^{n-1}}. \quad (6)$$

From Table 1 we note that the period may increase linearly with increasing grating thickness, have curvature, or a number of other profiles depending on the combination of aberrations present in the system.

Once a grating has been recorded with this spatially varying period it may be used as a reflecting Bragg grating for a probe beam propagating along the x -axis in Fig. 1. As each point of the beam will be subject to a different period (and therefore have a different reflectance) the total reflectance of the beam may be calculated by integrating over all of the points across the grating aperture:

$$R(\lambda) = \frac{\iint R(y, z, \lambda) I_p(y, z, \lambda) dy dz}{\iint I_p(y, z, \lambda) dy dz}. \quad (7)$$

Here R is the reflectance and I_p is the intensity of the probe beam being reflecting by the volume grating. In the simplest case where there is no spherical, coma x , or 30° trefoil aberrations (and assuming all higher order aberrations are negligible) we note there is no chirp of the period along the depth of the grating at a given point along the face. In this case the reflectance spectrum at a given point of the grating face can be written using Kogelnik's coupled-wave theory^{15,16} as

$$R(y, z, \lambda) = \frac{\sinh^2\left(\sqrt{S_0^2 - \Delta^2}\right)}{\cosh^2\left(\sqrt{S_0^2 - \Delta^2}\right) - \Delta^2 / S_0^2}, \quad (8)$$

where

$$S_0 = \frac{\pi \delta n t}{\lambda_B(y, z) \cos \theta_p} \quad (9)$$

is the strength of the grating and

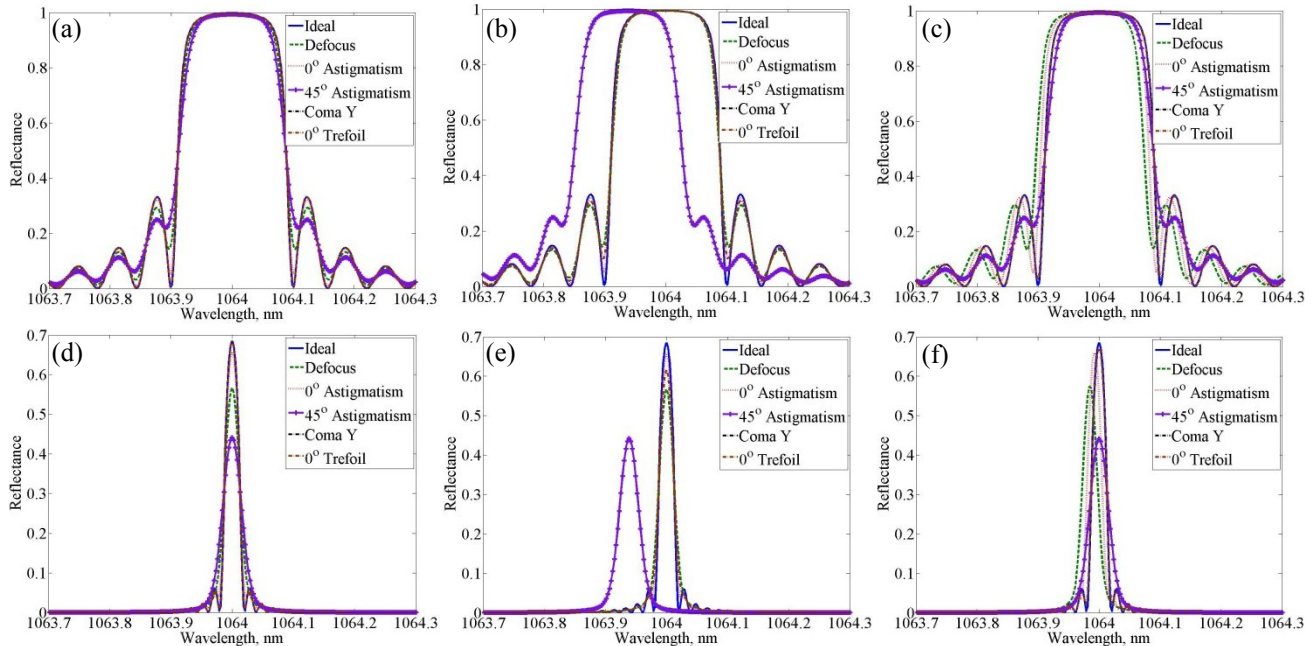


Fig. 2: Reflection spectrum of a 5 mm Gaussian beam in the presence of one wave of the indicated aberration for Grating A [(a), (b), (c)] and Grating B [(d), (e), (f)]. The location of the probe beam along the grating face is [(a), (d)]: $y' = z' = 0$, [(b), (e)]: $y' = 0.5, z' = 0$, and [(c), (f)]: $y' = 0, z' = 0.2$.

$$\Delta = 2\pi n_0 t \cos \theta_p \left(\frac{1}{\lambda} - \frac{1}{\lambda_B(y, z)} \right) \quad (10)$$

is the detuning from the Bragg condition. Here δn is the refractive index modulation, t is the thickness of the grating (along the x -axis), $\lambda_B = 2n_0\Lambda$ is the Bragg wavelength at a specific point, n_0 is the average refractive index at the Bragg wavelength, and θ_p is the deviation of the probe beam from normal incidence.

Due to the spatially varying nature of the grating one may reasonably conclude that several factors will influence the reflectance spectrum, including the length and strength of the grating, the position of the probe beam along the grating face, and the size of the probe beam. To determine the influence of these effects we simulate two gratings: a high efficiency, relatively thin grating (Grating A), useful in applications such as spectral beam combining, and a long grating with moderate diffraction efficiency (Grating B), which may be used in applications requiring narrow spectral widths. Grating A is designed such that it ideally has a 1064 nm resonant wavelength with $\delta n = 200$ ppm, and $t = 5.5$ mm. From Eqs. 8-10 this should give a diffraction efficiency of 99.4% and a spectral width of 178 pm. Grating B is designed for the same resonant wavelength, with $\delta n = 20$ ppm, and $t = 20$ mm, corresponding to a diffraction efficiency of 68.5% and a spectral width of 24 pm. To account for beam size and position, we use a 5 mm diameter Gaussian probe beam (a common size that is nevertheless large enough to have potentially significant differences in reflectance over the illuminated region) at normal incidence and examine three locations along the grating face: the center of the grating where the effects of aberrations are expected to be minimal, and halfway between the grating edge and center along the y and z axes. For 25 mm diameter recording beams interfering through a 10 mm recording medium the three probe locations correspond to: (a) $y = z = 0$, (b) $y = 6.25$ mm ($y' = 0.5$), $z = 0$, and (c) $y = 0, z = 2.5$ mm ($z' = 0.2$).

Fig. 2 shows the effects of one wave of a given aberration on the reflectance spectrum for both gratings. As expected, these aberrations have the least effect at the center of the grating, where the resonant wavelength is unchanged in all cases. However, the side lobes become at least partially washed out for both gratings and Grating B shows a reduction in peak diffraction efficiency as well as spectral broadening, with 45° astigmatism having the largest effect. The change in peak diffraction efficiency and spectral broadening are not noticeable in Grating A due to the wide initial spectral width, in which small changes at a given point are lost in the convolution of Eq. 7. When the probe beam is off-

center, there is also a change in resonant wavelength, equal in both gratings, by up to several tens of picometers, with 45° astigmatism having the largest effect when the beam is shifted on the y -axis and defocus having the largest effect when shifted on the z -axis.

In conclusion, we have determined that aberrations in recording beams can have significant adverse effects on an RBG due to the spatial dependence of the overlapped recording wavefronts. This results in a spatially varying resonant wavelength, which is problematic for spectral filtering, and the side lobes of the reflection spectrum are washed out, which reduces the efficiency of spectral beam combining. Spectral broadening and a reduction in peak diffraction efficiency are also present. However, the wider the initial spectral width of the grating, the less noticeable these effects will be. To determine the total degradation in spectral response that will be induced by a given recording setup the wavefront of the recording beams can be measured with a standard wavefront sensor and the impact of the measured aberrations can be calculated. If the aberrations reduce the spectral response beyond a desired tolerance, all optics should be aligned for on-axis use, and specialized optics such as aspherical or astigmatic lenses may be used as necessary to achieve the desired response.

REFERENCES

- [1] Sevian, A., Andrusyak, O., Ciapurin, I., Smirnov, V., Venus, G., and Glebov, L. B., "Efficient power scaling of laser radiation by spectral beam combining," *Opt. Lett.* **33**, 384-386 (2008).
- [2] Andrusyak, O., Smirnov, V., Venus, G., Rotar, V., and Glebov, L. B., "Spectral combining and coherent coupling of lasers by volume Bragg gratings," *IEEE J. Sel. Topics in Q. Electr.* **15**, 344-353 (2009).
- [3] Lægsgaard, J., "Control of fibre laser mode-locking by narrow-band Bragg gratings," *J. Phys. B: At. Mol. Opt. Phys.* **41**, 095401 (2008).
- [4] Jiao, Z., Liu, J., Lu, Z., Zhang, X., Poole, P. J., Barrios, P. J., and Poitras, D., "A C-band InAs/InP quantum dot semiconductor mode-locked laser emitting 403-GHz repetition rate pulses," *IEEE Phot. Tech. Lett.* **23**, 543-545 (2011).
- [5] Qiu, T., Suzuki, S., Schülzgen, A., Li, L., Polynkin, A., Temyanko, V., Moloney, J. V., and Peyghambarian, N., "Generation of watt-level single-longitudinal-mode output from cladding-pumped short fiber lasers," *Opt. Lett.* **30**, 2748-2750 (2005).
- [6] Sarangan, A. M., Huang, W. P., Li, G. P., and Makino, T., "Selection of transverse oscillation modes in tilted ridge DFB lasers," *J. Lightwave Tech.* **14**, 1853-1858 (1996).
- [7] Liu, Y., Chiang, K. S., and Chu, P. L., "Fiber-Bragg-grating force sensor based on a wavelength-switched self-seeded Fabry-Pérot laser diode," *IEEE Phot. Tech. Lett.* **17**, 450-452 (2005).
- [8] Chen, G., Liu, L., Jia, H., Yu, J., Xu, L., and Wang, W., "Simultaneous pressure and temperature measurement using Hi-Bi fiber Bragg gratings," *Opt. Comm.* **228**, 99-105 (2003).
- [9] Hieta, T., Vainio, M., Moser, C., Ikonen, E., "External-cavity lasers based on a volume holographic grating at normal incidence for spectroscopy in the visible range," *Opt. Comm.* **282**, 3119-3123 (2009).
- [10] Saikawa, J., Fujii, M., Ishizuki, H., and Taira, T., "High-energy, narrow-bandwidth periodically poled Mg-doped LiNbO₃ optical parametric oscillator with a volume Bragg grating," *Opt. Lett.* **32**, 2996-2998 (2007).
- [11] Chen, N., "Aberrations of volume holographic grating," *Opt. Lett.* **10**, 472-474 (1985).
- [12] Suzuki, Y., Mohri, J., Nakayama, K., Ando, M., Sakamoto, K., Yamauchi, M., Mizutani, Y., Yokouchi T., and Ejima, S., "Effect of Spherical Aberration on Fabrication of Fiber Bragg Gratings," *Jap. J. Appl. Phys.* **45**, 5035-5038 (2006).
- [13] Ma, M., Wang, X., and Wang, F., "Aberration measurement of projection optics in lithographic tools based on two-beam interference theory," *Appl. Opt.* **45**, 8200-8208 (2006).
- [14] Goodwin, E. and Wyant, J., [Field Guide to Interferometric Optical Testing], SPIE Press (2006).
- [15] Kogelnik, H. "Coupled wave theory for thick volume holograms," *Bell System Tech. J.* **45**, 2909-2944 (1969).
- [16] Glebov, L. B., Lumeau, J., Mokhov, S., Smirnov, V., and Zeldovich, B. Ya. "Reflection of light by composite volume holograms: Fresnel corrections and Fabry-Pérot spectral filtering," *J. Opt. Soc. Am. A* **25**, 751-764 (2008).